Mathematics and Computer Science
2018; 3(4): 93-99
http://www.sciencepublishinggroup.com/j/mcs
doi: 10.11648/j.mcs.20180304.13
ISSN: 2575-6036 (Print); ISSN: 2575-6028 (Online)

Heat and Mass Transfer of NH_3-H_2O Falling-Film Absorption on Horizontal Round Tube Banks

Nghia-Hieu Nguyen[1], Hiep-Chi Le[2, *], Quoc-An Hoang[3]

[1]Faculty of Heat & Refrigeration Engineering, Industry University of Ho Chi Minh City, Ho Chi Minh City, Vietnam

[2]Department of Heat & Refrigeration Engineering, Ho Chi Minh City University of Technology, VNU-HCM, Ho Chi Minh City, Vietnam

[3]Science Technology Office, Ho Chi Minh City University of Technology and Education, Ho Chi Minh City, Vietnam

Email address:

nguyenhieunghia@iuh.edu.vn (Nghia-Hieu N.), lechihiep@hcmut.edu.vn (Hiep-Chi Le), hanquoc@hcmute.edu.vn (Quoc-An H.)

[*]Corresponding author

To cite this article:

Nghia-Hieu Nguyen, Hiep-Chi Le, Quoc-An Hoang. Heat and Mass Transfer of NH_3-H_2O Falling-Film Absorption on Horizontal Round Tube Banks. *Mathematics and Computer Science*. Vol. 3, No. 4, 2018, pp. 93-99. doi: 10.11648/j.mcs.20180304.13

Received: July 12, 2018; **Accepted**: July 30, 2018; **Published**: August 23, 2018

Abstract: The absorption process has been confirmed as the most important process in absorption refrigeration machines in terms of improving their total efficiency. For this reason, absorber structures in general and heat and mass transfers in absorber in particular have attracted the interest of many researchers in this field. Commonly, the falling film absorber structure is the liquid mixture flows over tubes in a film mode. Mathematical model is developed for the falling film flowing on horizontal round tubes absorber derived from the mathematical model of the test volume element. The two-dimensional numerical simulation is written to solve partial differential equations predicting absorption efficiency. For evaluating the parameters which affect the coupled heat-mass transfer as NH_3-H_2O diluted solution flowing over horizontal round tubes absorb NH_3 vapor to become the higher concentration solution. The fields of velocity, temperature, concentration and thickness of the falling film solution varied by the input conditions of diluted solution and cooling water temperature flowing in the tube represented for a test volume element of the tube. The correlations which give the heat transfer coefficient and mass transfer coefficient in the absorption process in range of solution concentration $\omega = 28\% \div 31\%$, solution mass flow rate per unit tube length $\Gamma = 0.001 \div 0.015$ $kgm^{-1}s^{-1}$, coolant temperature $t_{water} = 28°C \div 38°C$ are set as two functions. The accuracy of numerical model and experiments are compared by the inlet, outlet the tube bundle of cooling water temperatures and absorber heat load. The absorber heat load deviation of the computing program $Q_{a\_cumpute}$ and experimental result Q_{a_meas} is 4.3%. The absorber heat load deviation of simulation result Q_{a_sim} and experimental result Q_{a_meas} is 12.3%. The overall heat transfer coefficient k used for simulation result of absorber heat load was taken from the relationship of the heat transfer coefficient $k = f(C; \Gamma; T) = f(0.308; 0.008; 306.3) = 0.863$ $kWm^{-2}K^{-1}$). The results were also evaluated with other similar studies by other authors. Based on these simulations, the theoretical studies were done for absorption refrigeration system in order to narrow the working area where the experiments later focused on. The results of this study will be the basis for subsequent application research of falling film absorbers.

Keywords: Absorption Refrigeration, NH_3-H_2O Solution, Absorber, Falling Film, Heat and Mass Transfer

1. Introduction

Heat exchanger plays an important role in chemical processing, refrigeration, petroleum refining, food industries and desalination as evaporators, condensers and absorbers. So falling film technology of heat exchanger has been widely researched by experts. Because compare with the flood exchanger, it provides higher heat transfer coefficient and smaller liquid inventory [1, 2]. And Horizontal-tube falling film absorbers can realise high heat and mass transfer rates with compact size and negligible pressure losses [3]. The absorber is usually the largest component in absorption cooling systems. An improvement in the absorption process leads to a reduction in area of the heat exchangers, and therefore a significant reduction in the costs of absorption chillers [4]. Falling film absorber is the most popular due to

many advantages of heat transfer efficiency, easy to assemble, easy to manufacture, especially well-suited to Vietnam conditions. This research focuses on the properties of motion, the coupled heat and mass transfer of falling film absorption on the horizontal tubes of the cooling tube bundle.

Two common pairs of working fluid (refrigerant-absorbent) in refrigeration absorption system are H_2O-LiBr and NH_3-H_2O. Testing absorber using dilute solution concentration (NH_3-H_2O) distributed evenly from top to form the falling film around the tubes of parallel tube layers, NH_3 vapor go pass through the tube layers from the absorber bottom [5-9]. Dilute solution absorb NH_3 vapor to become stronger solution generating the absorption heat flow. This heat flow go through the tube wall to the cooling water flowing in tubes and carry it away. The falling film covers only one part of the tube depends on the fluid distribution along the tube length and surface tension of the solution, as well as surface roughness of tube.

Solution concentration profile and temperature profile of the film leaving out the cooling tube bottom have decisive role in appropriate choice between adequate absorber size and system operation. Therefore, studying of the influence of solution flow rate, cooling water temperature, solution concentration inlet, and cooling water flow rate on heat and mass transfer coefficients are urgently needed for accurate thermal calculations and applications which is used for designing in falling film absorber.

2. Mathematical Model for a Test Volume

2.1. Model Description

A test volume element has 100% wetted ratio. 3D physical models become 2D physical model has dilute solution flow direction along the tube circumference by coordinate x. Film thickness direction is from the tube center by coordinate y. Any points on the film are determined by coordinate θ, y respectively.

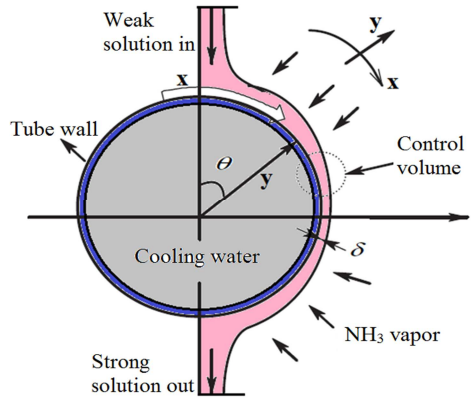

Figure 1. *2D physical model.*

Assumptions of 2D physical model

1. The flow is laminar and there are no interfacial waves;
2. Wettability of the solution on the tube surface is 100%;
3. Thermodynamic equilibrium exits at the interface between of solution film and vapor;
4. Heat transfer from interface to vapor phase is negligible;
5. The variation of film thickness due to absorption of NH_3 vapor is negligible;
6. Outside tube surface temperature equals the cooling water temperature.

2.2. Mathematical Description

The continuity, momentum, energy, transport equations of solution falling film on tube bundle are described 2D [10-13].

For a given solution mass flow rate per unit tube length $\Gamma = \dot{m}/L$ ($kgm^{-1}s^{-1}$). Film thickness (m) is expressed as equation (1).

$$\delta = \left[1 - \frac{3.\upsilon.\Gamma}{(WR).\rho.g.\sin\theta}\right]^{1/3} \tag{1}$$

Where υ is kinematic viscosity of solution (m^2s^{-1}) and WR is wetted ratio of the tube (%).

Velocity component u (ms^{-1}) along x direction is belong to flow direction as equation (2).

$$u = \frac{g.\sin\theta}{2.\upsilon}(2.\delta.y - y^2) \tag{2}$$

Velocity component v (ms^{-1}) along y direction is normal to flow direction as equation (3).

$$v = -\frac{g}{2.\upsilon}y^2\left[\frac{d\delta}{dx}\sin\theta + \frac{1}{R_o}(\delta - \frac{y}{3}).\cos\theta\right] \tag{3}$$

The phenomenon of coupled heat and mass transfer in steady state is discribed by energy transport equation (4) and spicies transport equation (5).

$$u\frac{\partial T}{\partial x} + v\frac{\partial T}{\partial y} = \alpha\frac{\partial^2 T}{\partial y^2} \tag{4}$$

$$u\frac{\partial \omega}{\partial x} + v\frac{\partial \omega}{\partial y} = D\frac{\partial^2 \omega}{\partial y^2} \tag{5}$$

Where α and β are thermal diffusivity (m^2s^{-1}) and mass diffusivity (m^2s^{-1}) of solution respectively, while T and ω are corresponding temperature and concentration of solution at the appropriate reference point.

Concentration and temperature boundary conditions at the inlet (6).

$$\begin{cases} x = x_{in} \\ 0 \le y \le \delta \end{cases} \rightarrow \begin{cases} T = T_{in} \\ \omega = \omega_{in} \end{cases} \tag{6}$$

Concentration and temperature boundary conditions at the tube wall surface (7).

$$\begin{cases} x_{in} \le x \le x_{out} \\ y = 0 \end{cases} \rightarrow \begin{cases} T = T_{wall} \\ \dfrac{\partial \omega}{\partial y} = 0 \end{cases} \tag{7}$$

Concentration and temperature boundary conditions at the liquid-vapor interface (8).

$$\begin{cases} x_{in} \le x \le x_{out} \\ y = \delta \end{cases} \rightarrow \begin{cases} \dot{m} = \dfrac{\rho.D}{(1-\omega_{\text{int}})}\dfrac{d\omega}{dy} & at\ y=\delta\ (concentration) \\ q = m'.h_{ab} = k_f \dfrac{dT}{dy} & at\ y=\delta\ (heat\ flow) \\ T_{\text{int}} = f(p,\omega_{\text{int}}) & at\ y=\delta\ (equivalent) \end{cases} \quad (8)$$

Where m' is calculated mass flux ($kgm^{-2}s^{-1}$), h_{ab} is heat of absorption (Jkg^{-1}) and k_f is thermal conduction conductivity of solution ($Wm^{-1}K^{-1}$).

Local heat transfer coefficients from interface to bulk solution along the film flow (9) and from bulb solution to tube wall surface along the film flow (10) in terms of Nusselt number.

$$Nu_{ib} = \frac{\alpha_{ib}.\delta}{k_f} = \frac{\delta}{(T_{\text{int}} - T_{sb})}\frac{dT}{dy} \qquad at\ y=\delta \qquad (9)$$

$$Nu_{\text{bwall}} = \frac{\alpha_{\text{bwall}}.\delta}{k_f} = \frac{\delta}{(T_{sb} - T_{\text{wall}})}\frac{dT}{dy} \qquad at\ y=0 \qquad (10)$$

Where α_{ib} and α_{bwall} are heat transfer coefficients from interface to bulk and from bulk to wall ($Wm^{-2}K^{-1}$), while T_{int}, T_{sb} and T_{wall} are temperatures at interface, bulk solution, and tube wall respectively.

Mass transfer coefficient from interface to bulk solution along the film flow (11) in terms of Sherwood number.

$$Sh = \frac{h_m}{D_{ab}} = \frac{m'.\delta}{D_{ab}.\rho.(\omega_{\text{int}} - \omega_{sb})} \qquad (11)$$

Where h_m is mass transfer coefficient from interface to bulk (ms^{-1}), D_{ab} diffusion coefficion of absorption (m^2s^{-1}).

Total heat transfer coefficient from bulk solution to cooling water ($Wm^{-2}K^{-1}$) can be expressed as (12).

$$\frac{1}{U} = \frac{1}{\alpha_{\text{bwall}}} + \frac{1}{\alpha_{\text{w}}} + \frac{\delta_{\text{wall}}}{\lambda_{\text{wall}}} \qquad (12)$$

Where α_{bwall} and α_{w} are convective heat transfer coefficients from bulk solution to wall and for cooling water ($Wm^{-2}K^{-1}$), while δ_{wall} and λ_{wall} are wall thickness of cooling tube (m) and thermal conductivity of tube wall ($Wm^{-1}K^{-1}$) respectively.

The physical domain has a complex geometry. Moreover, the film thicness is in micro-size vs half circumference length of the cooling tube is 0.0157 m. This ratio make the domain can not be meshed directly which must be transformed from sliding coordinate xy to non-dimentional coordinate εη making the computational domain rectangular.

3. Result and Discussion

Parameters used in this study are presented in table 1. Figure 2 shows the mass transfer phenomenon as NH_3 vapor is absorbed in order to become a stronger concentration solution.

Table 1. *Input parameters.*

Parameters	Values
Inlet temperature T_{in}	316 K
Inlet solution concentration ω_{in}	0.295
Absorber pressure p	2.8 bar
Solution density ρ	880 kgm^{-3}
Dynamic viscosity μ	3.95* 10^{-4} Nsm^{-2}
Solution flow rate Γ	0.008 $kgm^{-1}s^{-1}$
Out tube radius R_o	0.005 m
Thermal diffusivity α	6.7*10^{-8} m^2s^{-1}
Mass diffusivity D	4.4*10^{-9} m^2s^{-1}
Wall tube temperature T_{wall}	303 K
Thermal conductivity of solution k_f	0.384 $Wm^{-1}K^{-1}$

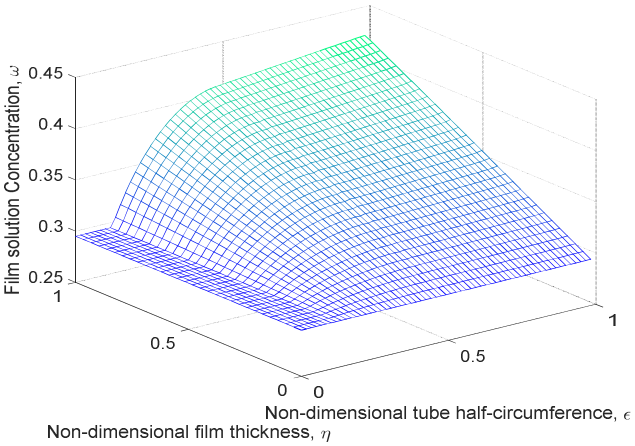

Figure 2. *Concentration profile, ω.*

Figure 2 is the three-dimensional distribution of the concentration ω in the solution film domain. Concentration of dilute solution when the solution has not contact the tube assumed without absorption phenomenon so the concentration equals the inlet concentration. Interface temperature is saturated to solution concentration. At tube wall, solution temperature equals wall temperature. When absorption phenomenon occurs, concentration of the liquid-vapor interface increases along ε-axis (x), then diffuses into the tube wall along η-axis (y). This absorption generates heat making liquid-vapor interface temperature increases along ε-axis (x). Due to the temperature difference between the interface and tube wall, heat transfer to the wall along axis η (y).

Average concentration of the film leaves the wall ω = 0.3537; increases 0.0587. Average temperature of the film coming in the tube is 317.6 K (44.5°C), average temperature of the film leaving tube is T = 304.8 K (31.7°C), decreases 12.8°C. Temperature of the liquid-vapor interface coming in the tube is 332 K (58°C), temperature of the liquid-vapor interface leaving the tube is T = 306.5 K (33.4°C), decreased 24.7°C. Difference temperature between liquid-vapor interface leaving the tube and the tube wall is 3.4°C.

3.1. The Effect of Solution Flow Rate on Heat and Mass Transfer

Input data as in table 1, tube wall temperature is 303 K, average local temperature at the inlet of falling film on tube is 325 K, solution flow rate Γ are changed: 0.001; 0.005;

0.008; 0.0113; 0.0146; 0.03 $kgm^{-1}s^{-1}$. Figures 3 and 4 show the variation of heat transfer coefficient and mass transfer coefficient with non-dimensional tube half circumference for different solution flow rates, while table 2 presents the thickness variation, the average local velocity, the average local concentration, the average local temperature, the heat transfer coefficient, the mass transfer coefficient of the film.

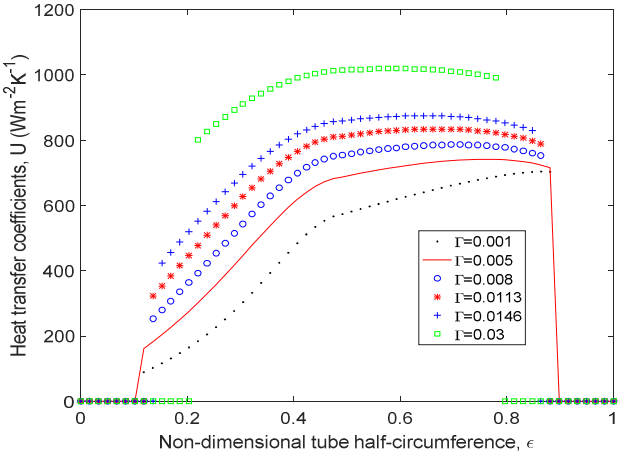

Figure 3. *Heat transfer coefficient, U $Wm^{-2}K^{-1}$.*

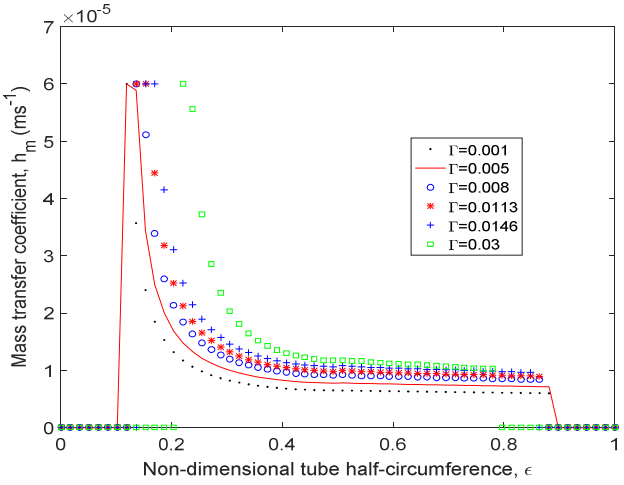

Figure 4. *Mass transfer of the film, h_m ms^{-1}.*

Figure 3 shows the heat transfer coefficient between the liquid-vapor interface and cooling water flowing in the tube U along ε-axis (x). These coefficients increase in the first quarter of the tube and decrease in the second quarter of tube. This shows absorption rate decreases as heat transfer coefficient decreases.

Figure 4 shows the change of the mass transfer coefficient along ε-axis (x). Mass transfer coefficient increases rapidly when the dilute solution just contact the tube wall, then decreases rapidly and fairly flat before leaving the tube wall. When solution flow rate increases, mass transfer coefficient increase, when the increase of flow rate is sizable (Γ = 0.0146 $kgm^{-1}s^{-1}$) or more, mass transfer increases very small.

Table 2. *The effect of solution flow rate.*

Γ $kgm^{-1}s^{-1}$	$\omega_{al\ o}$	$T_{al\ o}$ K	U $Wm^{-2}K^{-1}$	h_m ms^{-1} 10^{-5}
0.001	0.369	303.9	488.2	0.967
0.005	0.363	304.8	584.8	1.197
0.008	0.358	305.6	658.1	1.323
0.0113	0.354	306.5	719.1	1.467
0.0146	0.349	307.4	778.1	1.543
0.03	0.329	311.1	975.7	1.657

According to table 2, as solution flow rate distribution decreases 1%, average concentration of the film leaving the tube increases, heat transfer coefficient from interface to wall decreases 0.72%, heat transfer coefficient decreases significantly 0.56%; mass transfer coefficient decreases significantly 3.27%.

3.2. The Effect of Cooling Water Temperature on Heat and Mass Transfer

Input data as in table 1, solution flow rate distribution 0.008 $kgm^{-1}s^{-1}$, tube wall temperature are changed: 311; 309; 307; 305; 303; 301 (K). Figures 5 and 6 show the variation of average local concentration and average local temperature with non-dimensional tube half circumference for different tube wall temperatures.

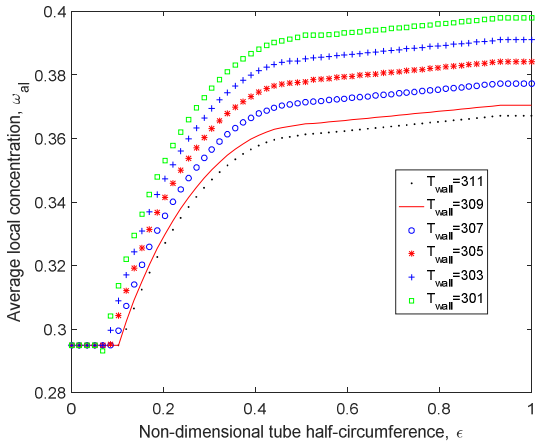

Figure 5. *Average local concentration, ω.*

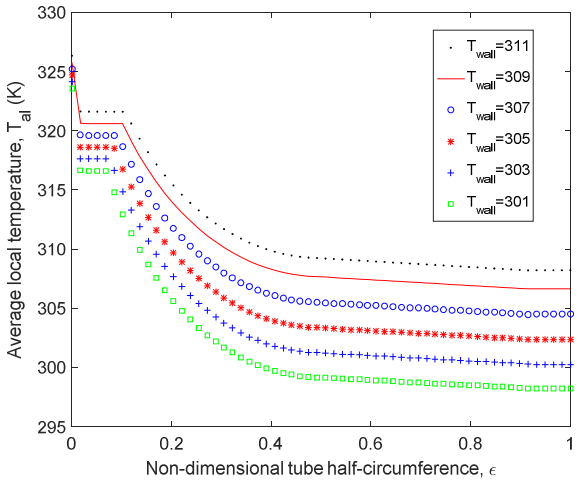

Figure 6. *Average local temperature, T K.*

When cooling water temperature decreases, average local concentration increases (Figure 5), average local temperature decreases (Figure 6).

Table 3. *The effect of cooling water temperature.*

T_{wall} K	ω_{al_o}	T_{al_in}/ T_{al_o} K	U $Wm^{-2}K^{-1}$	h_m ms^{-1} 10^{-5}
311	0.329	321/315	904	1.1688
309	0.332	320/313	926	1.2717
307	0.338	319/311	949	1.3713
305	0.344	318/309	969	1.4612
303	0.349	317/307	985	1.5398
301	0.355	316/305	900	1.6110

According to table 3, cooling water temperature decreases 1°C, average concentration of the film leaving the tube increases, average film temperature leaving the tube decreases, heat transfer coefficient increases 0.95%; mass transfer coefficient increases significantly 3.7%.

3.3. The Effect of Solution Concentration on Heat and Mass Transfer

Input data as in table 1, solution flow rate distribution 0.008 $kgm^{-1}s^{-1}$, tube wall temperature 305 K. Figures 7 and 8 show the variation of heat transfer coefficient and mass transfer coefficient with non-dimensional tube half circumference for different solution concentrations.

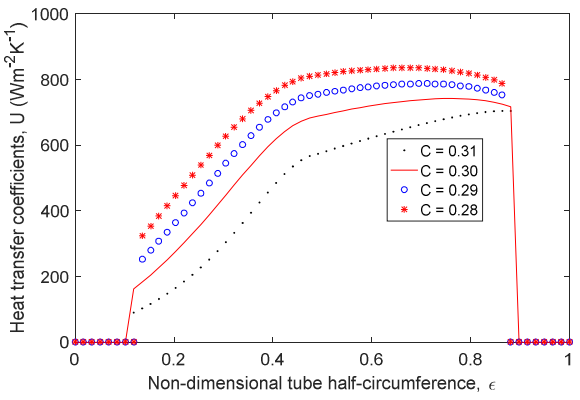

Figure 7. *Heat transfer coefficient, U $Wm^{-2}K^{-1}$.*

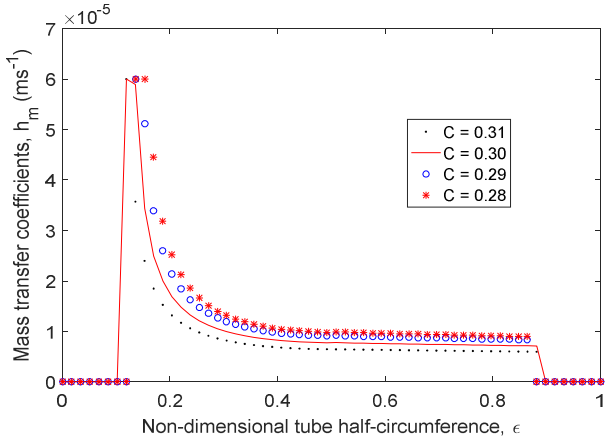

Figure 8. *Mass transfer coefficient, h_m ms^{-1}.*

The concentration of the film decreases, the heat transfer coefficient increases; mass transfer coefficient increases.

Table 4. *The effect of solution concentration.*

ω_i	ω_{al_o}	T_{al_o} K	U $Wm^{-2}K^{-1}$	h_m ms^{-1} 10^{-5}
0.31	0.367	303.4	704	1.1223
0.30	0.363	304.8	739	1.1736
0.29	0.356	305.2	775	1.2249
0.28	0.352	306.0	810	1.2753

According to table 4, as concentration of the film decreases 1%, average concentration of the film leaving the tube increases, average film temperature leaving the tube increases, heat transfer coefficient increases 1.46%; mass transfer coefficient increases 1.39%.

3.4. Heat and Mass Transfer Coefficients

A correlation which gives heat transfer coefficient and mass transfer coefficient in the absorption process in range of solution concentration ω = 28% ÷ 31%, solution mass flow rate per unit tube length Γ = 0.005 ÷ 0.015 ($kgm^{-1}s^{-1}$), coolant temperature t = 28°C ÷ 38°C are set as two funtions.

These functions are derived to estimate the absorber capacity and mass flow rate of NH_3 vapor into NH_3-H_2O solution.

$$U = A + B*\omega + C*\Gamma + D*T_{wall} + G*\Gamma^2 + K*T_{wall}^2 \quad (13)$$

$$h_m = A + B*\omega + C*\Gamma + D*T_{wall} + G*\Gamma^2 + K*T_{wall}^2 \quad (14)$$

Table 5. *Constant of U and h_m correlation.*

Constant	U $Wm^{-2}K^{-1}$	h_m ms^{-1}
A	-16374,2444	-0.0009451752
B	-3999,9999	-0.0000629999
C	47142,4463	0.0006066080
D	126,7608	0.00000686285
G	97578,4861	-0.0120566076
K	-0,2211	-0.0000000120

Total heat transfer coefficient and mass transfer coefficient as functions of the initial solution concentration, solution mass flow rate per unit tube length, and cooling water temperature are derived as U = f(ω; Γ; T) = f(0.30; 0.008; 306) = 0.863 $kWm^{-2}K^{-1}$; h_m = f(ω; Γ; T)= f(0.30; 0.008; 306) = 1.45*10^{-5} ms^{-1} respectively.

3.5. Evaluation of Numerical and Experimental Result

Figure 9 shows the measured state point values for a specific working condition. The measured value of absorber heat load Q_{a_meas} = 3.270 kW is compared with the computed value $Q_{a\_compute}$ and numerical model Q_{a_sim}.

The input for the machine compution program are the condensing temperature t_c = 30.2°C, absorbing temperature of strong solution leaving the absorber t_a = 36°C, evaporating temperature t_e = -19°C, and the heat supply capacity Q_g = 3.762 kW. The optimal generating temperature will be t_g = 120°C.

Heat flows of the components: evaporator, condenser, absorber, generator, rectifier, work input to the solution pump, coefficient of performance are Q_e = 1.52 kW; Q_c =

1.727 kW; Q_a = 3.412 kW; Q_g = 3.762 kW; Q_r = 0.41 kW; Q_{p_out} = 0.362 kW; COP = 0.413 respectively. The heat load of the absorber $Q_{a\_compute}$ = 3.412 kW.

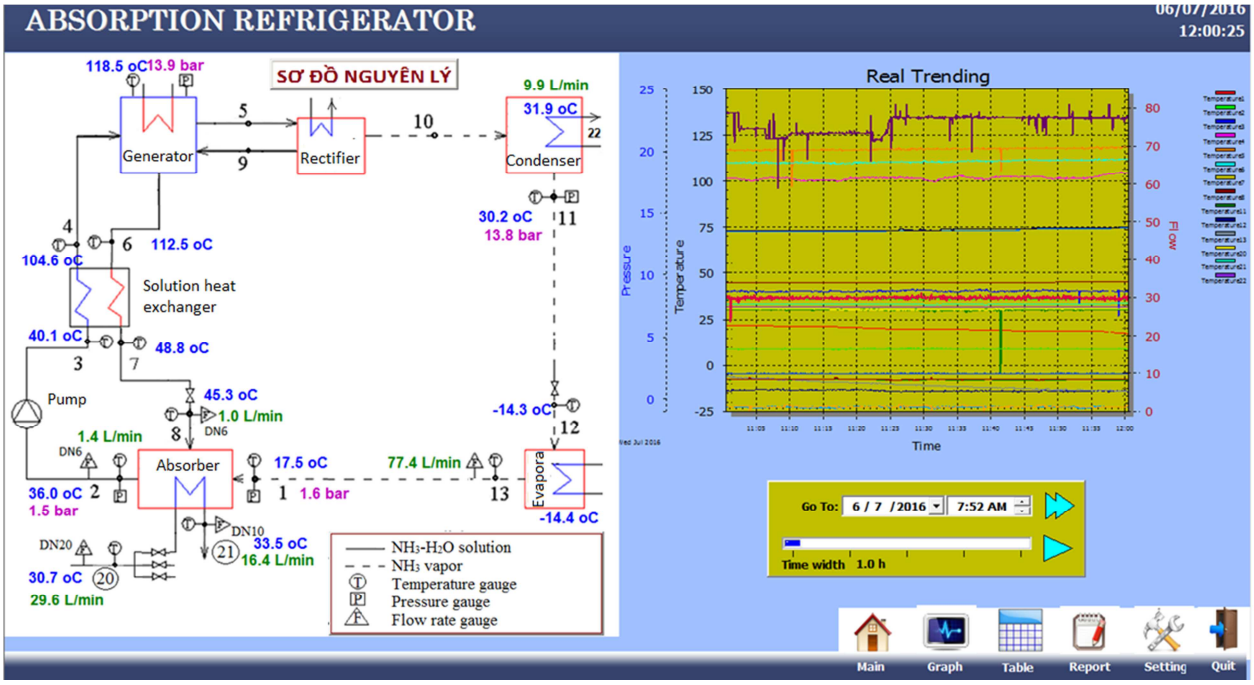

Figure 9. *Measured state point values.*

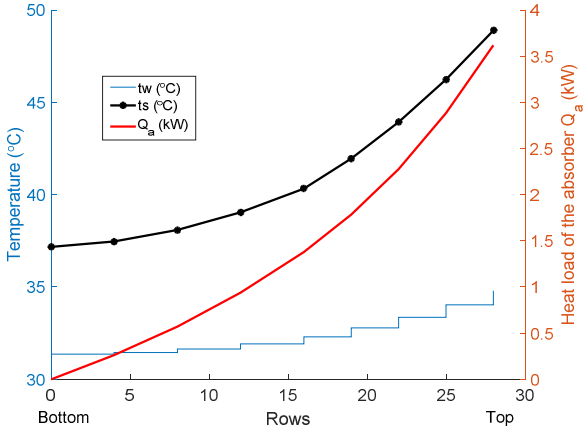

Figure 10. *Variation of temperature and heat load.*

Figure 10 depicts the variation of the simulated value of absorber Q_{a_sim} = 3.671 kW, the solution average temperature ts, water coolant tw along the horizontal tube-type falling film absorber design. While water coolant flows in the upward direction. The heat transfer coefficient is approximately constant U = 863 $Wm^{-2}K^{-1}$.

Table 6. *Numerical and experimental heat load of the absorber.*

Head load	Value (kW)	Deviation (%)
Q_{a_meas}	3.270	0
$Q_{a\_compute}$	3.412	4.3
Q_{a_sim}	3.671	12.3

The heat transfer coefficient and mass transfer coefficient as funtions of the initial solution concentration, solution mass flow rate per unit tube length, and cooling water temperature are derived as U = f(ω; Γ; T) = f(0.308; 0.008; 306.3) = 0.863 $kWm^{-2}K^{-1}$; h_m = f(ω; Γ; T)= f(0.308; 0.008; 306.3) = 1.45*10^{-5} ms^{-1} respectively.

Table 7. *Compare with other literatures.*

Analysis	U	h_m	Note
[14]	545-940		D_o = 1.575; D_i = 1.168, m = 0.0151 ÷ 0.0266, t = 52 & 81; ω = 28 ÷ 35.
[15]	540-1160		D_o = 1.575; D_i= 1.168, Γ = 0.00138÷0.005
[16]	571-831	2.19*10^{-5} ÷ 3.22*10^{-5}	D_o = 15.88 or 12.7 or 9.52, Sim. Γ = 0.008 ÷ 0.05, Exp. Γ = 0.0143 ÷ 0.03
[17]	753-1853	0.55*10^{-5} ÷ 3.31*10^{-5}	D_o = 9.5
Present study	488 ÷ 976	0.967*10^{-5} ÷ 1.65*10^{-5}	ω = 30%; T_w = 306.3 K; Γ = 0.001 ÷ 0.03

In addition, heat transfer and mass transfer coefficients of this research are compared with previous studies. Sangsoo Lee, Lalit Kumar Bohra, Srinivas Garimella, Ananda Krishna Nagavarapu [17] found heat transfer coefficient U = f(C; Γ; P) = f(0.25; 0.008; 2.5) = 0.88 $kWm^{-2}K^{-1}$ and mass transfer coefficient h_m = f(C; Γ; P) = f(0.25; 0.008; 2.5) = 1.65*10^{-5} ms^{-1}. Correlations of heat transfer and mass transfer coefficients of the absorption process to: (i) solution concentration ranging from 28% to 31%, (ii) solution mass flow rate per unit tube length ranging from 0.001 $kgm^{-1}s^{-1}$ to 0.03 $kgm^{-1}s^{-1}$) and (iii) cooling water temperature ranging from 301 K to 311 K were established.

4. Conclusion

Solution flow rate increases, average local concentration of the film decreases, average local temperature increases. Heat transfer coefficient increases strongly, mass transfer coefficient increases. When increasing of flow rate is sizable $\Gamma = 0.0146$ $kgm^{-1}s^{-1}$ or more, mass transfer increases very small.

The effects of the solution concentration $\omega = 28\% \div 31\%$, solution mass flow rate per unit tube length $\Gamma = 0.001 \div 0.015$ $kgm^{-1}s^{-1}$, cooling water temperature, and cooling water $t_w = 28°C \div 38°C$ on the heat transfer coefficient U $Wm^{-2}K^{-1}$ and mass transfer coefficient h_m ms^{-1} of the absorption process were:

a) As solution flow rate distribution decreases 1%, heat transfer coefficient decreases significantly 0.56% and mass transfer coefficient decreases significantly 3.27%.
b) As cooling water temperature decreases 1°C, heat transfer coefficient increases 0.95%; mass transfer coefficient increases significantly 3.7%.
c) As concentration of the film decreases 1%, heat transfer coefficient increases 1.46%; mass transfer coefficient increases 1.39%.

Two functions giving heat transfer coefficient and mass transfer coefficient in the absorption process in range of solution concentration $\omega = 28\% \div 31\%$, solution mass flow rate per unit tube length $\Gamma = 0.001 \div 0.03$ $kgm^{-1}s^{-1}$, coolant temperature $t_{water} = 28°C \div 38°C$ are set as (13) and (14).

This research did not receive any specific grant from funding agencies in the public, commercial, or not-for-profit sectors.

References

[1] Jingdong Chena, Jili Zhanga, Zhijiang Hua, Zhixian Maa, "Falling Film Transitions on Horizontal Enhanced Tubes: Effect of Tube Spacing," Procedia Engineering 205, 1542–1549 (2017).

[2] Christos N. Markides, Richard Mathie, Alexandros Charogiannis, "An experimental study of spatiotemporally resolved heat transfer in thin liquid-film flows falling over an inclined heated foil," International Journal of Heat and Mass Transfer 93, 872–888 (2016).

[3] Niccolò Giannetti, Andrea Rocchetti, Seiichi Yamaguchi, Kiyoshi Saito, "Heat and mass transfer coefficients of falling-film absorption on a partially wetted horizontal tube," Int. J. of Thermal Sciences 126, 56–66 (2018).

[4] María E._Alvarez, Jos_e A. Hern_andez, Mahmoud Bourouis, "Modelling the performance parameters of a horizontal falling film absorber with aqueous (lithium, potassium, sodium) nitrate solutionusing artificial neural networks," Energy 102, 313-323 (2016).

[5] Xavier Daguenet-Fric, Paul Gantenbein, Jonas Müller, "Benjamin Fumey, Robert Weber, Seasonal thermochemical energy storage: Comparison of the experimental results with the modelling of the falling film tube bundle heat and mass exchanger unit," Renewable Energy 1-12 (2016).

[6] A. V. Bobylev, V. V. Guzanov, O. M. Heinz, S. M. Kharlamov, A. Z. Kvon, D. M. Markovich, "Characterization of 3-D wave flow regimes on falling liquid films," International Journal of Multiphase Flow, Volume 99, Pages 474-484 (2018).

[7] Beethoven Narváez-Romo, Marx Chhay, Elí W. Zavaleta-Aguilar, José R. Simões-Moreira, "A Critical Review of Heat and Mass Transfer Correlations for LiBr-H_2O and NH_3-H_2O Absorption Refrigeration Machines Using Falling Liquid Film Technology," Applied Thermal Engineering, Volume 123, Pages 1079-1095 (2017).

[8] Delphine Triché, Sylvain Bonnot, Maxime Perier-Muzet, François Boudéhenn, Hélène Demasles, Nadia Caney, "Experimental and numerical study of a falling film absorber in an ammonia-water absorption chiller", International Journal of Heat and Mass Transfer 111, 374–385 (2017).

[9] Qiang Zhang, Yide Gao, "Analytical solution of velocity for ammonia-water horizontal falling-film flow", Applied Thermal Engineering, Volume 101, Pages 131-138 (2016).

[10] Niccolo Giannetti, Andrea Rocchetti, Kiyoshi Saito, Seiichi Yamaguchi, "Irreversibility analysis of falling film absorption over a cooled horizontal Tube," International Journal of Heat and Mass Transfer 88, 755–765 (2015).

[11] V. D. Papaefthimiou, I. P. Koronaki, D. C. Karampinos, E. D. Rogdakis, "A novel approach for modelling LiBr- H_2O falling film absorption on cooled horizontal bundle of tubes," Int. J. of refrigeration 35, p. 1115-1122 (2012).

[12] L. Harikrishnan, Shaligram Tiwari, M. P. Maiya, "Numerical study of heat and mass transfer characteristics on a falling film horizontal tubular absorber for R-134a-DMAC," International Journal of Thermal Sciences 50, p. 149-159 (2011).

[13] Conlisk AT, Mao J., "Nonisothermal absorption on a horizontal cylindrical tube-1. The film flow," Chemical engineering science, 51, p. 1275-1285, 1996.

[14] Meacham, J. M. G., Srinivas, *Ammonia-Water Absorption Heat and Mass Transfer in Microchannel Absorbers with Visual Confirmation,* ASHRAE 2004. 110 (1): p. 525-532.

[15] Srinivas Garimella, Matthew D. Determan, J. MarkMeacham, Sangsoo Lee, Timothy C. Ernst, "Microchannel component technology for system-wide application in ammonia/water absorption heat pumps," International Journal of Refrigeration, 34 (5): p. 1184-1196 (2011).

[16] Phan, T. T. (PhD. Thesis), *Performance of Horizontal Tube Absorber with Variation of Tube Diameter*, 2007, Pukyong National University [Thailand].

[17] Sangsoo Lee, Lalit Kumar Bohra, Srinivas Garimella, Ananda Krishna Nagavarapu, "Measurement of absorption rates in horizontal-tube falling-film ammonia-water absorbers," International Journal of Refrigeration, 35 (3): p. 613-632 (2012).